ELUCIDATING BRAIN CONNECTIVITY NETWORKS IN MAJOR DEPRESSIVE DISORDER USING CLASSIFICATION-BASED SCORING

Matthew D. Sacchet[1,2], Gautam Prasad[2,3], Lara C. Foland-Ross[2], Paul M. Thompson[3], Ian H. Gotlib[1,2]
[1]Neurosciences Program, and [2]Department of Psychology, Stanford University, Stanford, CA, USA
[3]Imaging Genetics Center, Inst. for Neuroimaging and Informatics, Keck Sch. of Med. of USC, Los Angeles, CA, USA

ABSTRACT

Graph theory is increasingly used in the field of neuroscience to understand the large-scale network structure of the human brain. There is also considerable interest in applying machine learning techniques in clinical settings, for example, to make diagnoses or predict treatment outcomes. Here we used support-vector machines (SVMs), in conjunction with whole-brain tractography, to identify graph metrics that best differentiate individuals with Major Depressive Disorder (MDD) from nondepressed controls. To do this, we applied a novel feature-scoring procedure that incorporates iterative classifier performance to assess feature robustness. We found that *small-worldness*, a measure of the balance between global integration and local specialization, most reliably differentiated MDD from nondepressed individuals. Post-hoc regional analyses suggested that heightened connectivity of the subcallosal cingulate gyrus (SCG) in MDDs contributes to these differences. The current study provides a novel way to assess the robustness of classification features and reveals anomalies in large-scale neural networks in MDD.

Index Terms— Major Depressive Disorder (MDD), graph theoretical analysis, machine learning, support vector machine (SVM), small-world

1. INTRODUCTION

Major Depressive Disorder (MDD) is one of the most prevalent and costly psychiatric disorders [1]. Understanding the neural foundations of MDD is critical for improving the prevention, detection, and treatment of this debilitating disorder.

Recently there has been considerable interest in using tools from computer science and mathematics in human neuroscience applications. For example, graph theory and machine learning techniques are being used to characterize large-scale network structure of the brain and to classify individuals into diagnostic groups based on measures of brain structure and function.

Graphs describe brain networks as mathematical structures formed by pairwise relations (called 'edges') between brain regions ('nodes'). In human neuroscience, edges (or *connections*) are most often derived from functional or diffusion-based relations between regions. Complex network measures derived from graph theoretical analyses can be used to characterize the human brain. They are reliable, easy to compute, and can be related to other measures (e.g., behavior or disease), e.g., to reveal anomalies in neurological and psychiatric disorders [2].

Several studies have used graph theoretical analyses to characterize large-scale brain networks in MDD. Different methods have been applied to assess brain networks in these studies: two studies used resting-state functional magnetic resonance imaging (fMRI; [3,4]), another examined synchronization among electroencephalography (EEG) electrodes [5], and the most recent study reported correlations between regional white-matter volumes [6].

The branch of computer science known as machine learning is concerned with the development of algorithms that can 'learn' patterns in data that can be used for predictive modeling or classification of data into groups. Machine learning techniques are multivariate, and can identify key features in dataset and how they interact. This makes them particularly amenable to neuroscience problems, given the complexity of the human brain.

Machine learning has been applied to human brain imaging data to classify disease states and optimize treatment selection [7]. In MDD, diagnosis and treatment rely largely on self-report and observation of clinical symptoms. In contrast, brain metrics, in conjunction with machine learning, may help in the diagnosis and treatment of this disorder. Indeed, recent diagnostic and treatment selection classification in the context of MDD has been promising [7], and one study used tractography-based connectivity to successfully classify depressed individuals [8]. Notably, however, that study did not use common graph metrics.

In the current study, nine common graph metrics were used as features for support-vector machine classification and scored based on their ability to differentiate depressed from nondepressed individuals. This approach may yield a more nuanced understanding of differences in networks than does univariate testing of single features. Furthermore, we used regional network analyses to discover regional differences that might underlie observed group differences in global graph metrics.

978-1-4673-1961-4/14/$31.00 ©2014 IEEE

2. METHODS

2.1 Participants

Fourteen MDD and 18 age-matched control (CTL) participants (all female) underwent diffusion-weighted imaging (DWI) and high-resolution anatomical (T1-weighted) magnetic resonance imaging. The Stanford University IRB approved the protocol and written informed consent was collected before data acquisition.

2.2 DWI and MRI Data Acquisition

Imaging data were acquired using a 3T Discovery MR750 (GE Medical Systems, Milwaukee, WI, USA), at the Center for Neurobiological Imaging at Stanford University. The DWI scan utilized a diffusion-weighted, dual spin-echo, single-shot, echo-planar imaging sequence and consisted of 64 2-mm thick slices in 96 unique directions (with b = 2000 s/mm^2), with voxel resolution 2x2x2 mm^3. The duration of this scan was 15 min 1 s. High-resolution anatomical scans were collected for anatomical localization (sagittal spoiled gradient sequence [SPGR], 0.9x0.9x0.9 mm^3 resolution).

2.3 Tractography and Cortical Segmentation

DWI data were preprocessed using FSL's eddy correction procedure [9]. Tractography was estimated from these eddy-corrected images using an optimized global probabilistic method [10,11]. This method was used to estimate 35,000 fibers for each subject. The freely available software, FreeSurfer (surfer.nmr.mgh.harvard.edu) was used for cortical reconstruction and segmentation of the T1-weighted images. This resulted in 34 unique cortical regions per hemisphere (68 total). These cortical regions were then dilated to ensure their intersection with white matter, to create a tractography-based connectivity matrix. The high-resolution anatomical images were registered to the raw fractional anisotropy (FA) image via the automatic registration toolkit (ART; [12,13]). ART first computes an affine and then a nonlinear transformation. These transforms were used to transform the enlarged cortical segmentations to raw DWI space.

2.4 Connectivity Matrix Computation

Connectivity matrices were created on a subject-by-subject basis by assessing the number of fibers that intersected pairs of cortical ROIs. This was done by combining, in the raw DWI space, the dilated cortical ROIs and tractography fibers. Each connectivity matrix was 68x68 (one row/column per ROI), with each element representing the raw number of intersecting fibers. These connectivity matrices were normalized so that their elements ranged from 0 to 1. Matrices were then thresholded to maintain the top 25% most strongly weighted edges, and binarized to set all remaining non-zero weights to 1. We selected 0.25 for the binarizing threshold as it has been suggested to be biologically plausible [14]. Binarization and all subsequent graph analyses were conducted using the freely available Brain Connectivity Toolbox [2].

2.5 Graph Metric Calculation

Nine graph metrics (*global efficiency*, *transitivity*, *path length*, *assortivity*, *modularity*, *small-worldness*, *flow coefficient*, *total flow*, and *betweenness*) were selected as features based on their ability to characterize whole-brain network characteristics (see [2] for equations and details). All metrics were computed from the 0.25 thresholded, binarized matrices, *modularity* was calculated as the average of ten iterations due to variability in the algorithm, and *small-worldness* was computed from *transitivity* and *path length* normalized relative to 10 randomized iterations of the given metric computed from a random network (with the same degree distribution as the original).

2.6 Support Vector Machine (SVM) Classification

SVM classifiers were trained to discriminate between graph metrics from the depressed and nondepressed participants. A leave-one-out cross-validation approach was used to access classifier accuracy performance. SVM training and testing was conducted using MATLAB (the Mathworks, Natick, MA, USA).

2.7 Assessment of SVM Success

Classification was performed for all possible combinations of the nine graph-metric features (i.e., 2^9 – zero feature set = 511 unique sets). To assess SVM performance, the number of single tests reaching significance (i.e., for a single sign test, 22 correct of 32 classifications reaches p = 0.0501) was tested in a binomial test with the assumption that only 5% of the 511 tests would reach significance under the null hypothesis; that is, that the SVM did not perform better than chance.

2.8 Identifying the Most Robust SVM Features

To assess how robust each feature was, we aggregated the accuracies for all SVM iterations that included a given feature. Next, permutation-based *t*-tests (100,000 iterations shuffling subjects by group status) were used to assess differences between accuracies associated with different features. This identified the graph metric that most robustly differentiated MDD from nondepressed individuals.

2.8 Regional Analysis of Neural Networks

To identify group differences in the neural networks, the numbers of neighbors for each region were compared between groups using permutation-based *t*-tests.

2.9 Correction for Multiple Comparisons

When appropriate, a False Discovery Rate (FDR; q = 0.05) procedure was used for multiple comparison correction [15].

TABLE 1
GRAPH METRICS

Graph Metric	CTL		MDD		*p*-value*
	M	*SD*	*M*	*SD*	
Global Efficiency	0.590	0.006	0.593	0.004	0.074
Transitivity	0.548	0.012	0.543	0.548	0.187
Path Length	1.916	0.029	1.907	0.019	0.314
Assortativity	-0.062	0.022	-0.065	0.038	0.822
Modularity	0.334	0.042	0.354	0.039	0.167
Small World	1.548	0.039	1.575	0.040	0.067
Flow Coefficient	0.329	0.013	0.339	0.013	0.039
Total Flow	1.441	4.592	1.441	3.962	0.991
Betweenness	62.921	2.649	62.559	1.492	0.659

Graph metrics by group. MDD = Major Depressive Disorder; CTL = control; *M* = mean; *SD* = standard deviation; **p*-value calculated from permutation *t*-test, no test reached significance after FDR correction.

3. RESULTS

3.1 Graph Metrics Between Groups

Permutation *t*-tests between graph metrics across groups did not reveal significant differences after correction for multiple comparisons (**Table 1**).

3.2 SVM Accuracy

For a single SVM iteration, 22 correct group classifications out of 32 classifications was considered significant using the sign test. Of the 511 SVM iterations, 228 iterations classified 22 or more individual correctly (binomial test: $p < 0.001$).

3.3 SVM Accuracy by Graph Metric

To assess the most robust graph metric, we compared the accuracies of SVM iterations associated with different metrics (Methods section 2.8; **Table 2**). *Small-worldness* was the most robust metric; *flow coefficient* was the graph metric that exhibited the next highest mean accuracy (*small-worldness*: *M* = 0.6888; *SD* 0.063; *Flow Coefficient*: *M* = 0.6628; *SD* 0.069; permutation *t*-test: $p < 0.001$).

3.4 Most Robust SVM Feature

Small-worldness was the most robust feature included in the SVM iterations. The aggregate accuracies associated with *small-worldness* were significantly different from 50% ($t(255) = 9.1$, $p < 0.001$). The SVM iteration only including *small-worldness* (a single feature) was not significant (59.4% accuracy; sign test: $p < 0.40$). The MDD group exhibited a (nonsignificantly) larger mean *small-world* organization than did the control group (MDD: *M* = 1.5747, *SD* = 0.0402; CTL: *M* = 1.5477, *SD* = 0.0393).

3.5 Regional Brain Differences

In seven brain regions, the MDD and CTL participants differed in degree at the $p < 0.05$ level; after FDR correction for multiple comparisons, only three tests remained significant: left rostral anterior cingulate, right inferior parietal cortex, and right *pars orbitalis* (**Table 3; Figure 1**).

TABLE 2
CLASSIFICATION ACCURACIES

Graph Metric	Accuracy *M*	*SD*	Number of SVMs*
Global Efficiency	0.6575	0.079	122
Transitivity	0.6575	0.088	135
Path Length	0.6539	0.083	123
Assortativity	0.6440	0.093	118
Modularity	0.6576	0.082	122
Small World	0.6888	0.063	169
Flow Coefficient	0.6628	0.069	132
Total Flow	0.6625	0.087	134
Betweenness	0.6492	0.088	115

SVM classification accuracies by graph metric feature; Number of SVMs = total number of SVMs in which p = 0.05 was reached, out of a total of 256 iterations; *binomial test all p-values < 0.001.

TABLE 3
REGIONAL CONNECTEDNESS

Region	CTL		MDD		p-value*
	M	*SD*	*M*	*SD*	
L. Banks S. Temp. Sulc.	15.6	2.3	13.1	3.4	0.014
L. Entorhinal	3.7	2.9	7.3	3.5	0.003
L. Ros. Ant. Cingulate	20.5	1.2	22.1	1.3	0.002**
L. Temporal Pole	5.8	2.1	7.4	1.6	0.024
R. Inferior Parietal	21.4	1.9	18.2	1.7	< 0.001**
R. Lateral Occipital	17	1.7	15.7	1.0	0.021
R. *Pars Orbitalis*	5.5	0.7	6.6	1.1	< 0.001**

Regional connectedness by group. *SD* = standard deviation; *M* = mean; *p-value calculated from two-tailed permutation *t*-test; ** indicates significance after FDR correction ($q = 0.05$); L. = Left; R. = right; Banks S. Temp. Sulc. = Banks of the superior temporal sulcus; Ros. Ant. Cingulate = Rostral anterior cingulate.

6. DISCUSSION

We found that the *small-worldness* of the brain's structural network most robustly differentiated individuals with MDD from nondepressed controls. Post-hoc regional analyses suggest that specific brain regions contribute to these differences. Importantly, neither *t*-tests nor SVMs with a single graph metric feature were able to reliably differentiate groups.

Even though *small-worldness* was the most robust graph metric feature, the inclusion of additional SVM features improved classification accuracy (compared to an SVM with a single *small-world* feature, and to results of group differences in *small-worldness* tested using *t*-tests). This points to the multivariate advantages of SVM, which may be better able to differentiate groups than typical group comparisons that assess differences in a single brain metric.

Depressed individuals had increased *small-world* organization compared to nondepressed individuals. *Small-worldness* measures the balance between local specialization and global integration, so increased *small-world* organization may relate to facilitated processing in networks responsible for symptoms associated with MDD, for example, negative emotional and ruminative processing. Future research should assess the contribution of specific nodes to the *small-world* metric.

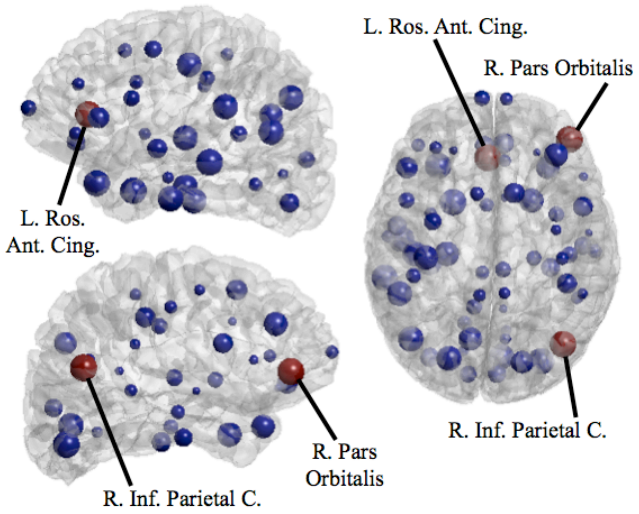

FIGURE 1.
REGIONAL CONNECTEDNESS
Upper left image is view from the left, bottom left image is view from the right, and the right image is the view from above. Blue spheres indicate non-significant statistical tests. Red spheres indicate statistically significant tests (FDR corrected, q = 0.05). The size of the sphere indicates the magnitude of p-value (displayed as 1 - p-value). L. Ros. Ant. Cing. = Left Rostral Anterior Cingulate; R. Inf. Parietal C. = Right Inferior Parietal Cortex; R. Pars. Orbitalis = Right Pars Orbitalis. The BrainNet Viewer was used for visualization (http://www.nitrc.org/projects/bnv/).

Small-world organization is calculated as the ratio of *transitivity* (or clustering coefficient) to *path length* (characteristic path length). Neither of these metrics, individually, differentiated the MDD and CTL groups (Table 1), and they were less able to differentiate groups across SVM iterations than was *small-worldness* (Table 2). Thus, the ratio of *transitivity* to *path length*, as computed in the *small-world* metric, is more informative for differentiating groups than either metric alone.

Prior studies found decreased *small-world* organization associated with depression [3,5,6]. This inconsistency with the current results may be because other imaging modalities were used to compute connectivity metrics (resting state fMRI [3], EEG synchronization [5], white-matter correlations [6]). Future research should attempt to relate graph metrics from different neuroimaging modalities.

Regional graph analyses suggest that MDDs differed from nondepressed individuals in the number of neighbor connections of certain regions. More specifically, MDDs exhibited more neighboring connections associated with rostral anterior cingulate cortex and the orbital part of the right inferior frontal gyrus, and less connectivity for the inferior parietal cortex. Notably, the rostral anterior cingulate cortex FreeSurfer cortical ROI primarily includes the subcallosal cingulate gyrus (SCG), a region of theoretical importance in the pathophysiology of MDD (see [16] for review).

In conclusion, the current study provides the first evidence that common tractography-based graph metrics may help in the classification of MDD, that *small-worldness* differentiates depressed from nondepressed individuals, and that altered SCG, right *pars orbitalis*, and right inferior parietal cortex connectivity may contribute to these large-scale network differences.

7. REFERENCES

[1] R. C. Kessler, and P.S. Wang, The epidemiology of depression. In I.H. Gotlib & C.L. Hammen (Eds.), Handbook of Depression, 2nd Edition. Guildford Press, New York, New York, 2009.
[2] M. Rubinov and O. Sporns, "Complex network measures of brain connectivity: Uses and interpretations," *NeuroImage*, vol. 52, pp. 1059-1069, 2010.
[3] C. Jin *et al.*, "A preliminary study of the dysregulation of the resting networks in first-episode medication-naïve adolescent depression," *Neurosci. Lett.*, vol. 503, pp. 105-109, 2011.
[4] J. Zhang *et al.*, "Disrupted brain connectivity networks in drug-naïve, first-episode major depressive disorder," *Biol Psychiatry*, vol. 70, pp. 334-342, 2011.
[5] S. J. Leistadt, N. Coumans, M. Dumont, J. P. Lanquart, C. J. Stam, and P. Linkowski, "Altered sleep brain functional connectivity in acutely depressed patients," *Hum Brain Mapp*, vol. 30, pp. 2207-2219, 2009.
[6] M. K. Singh *et al.*, "Anomalous gray matter structural networks in major depressive disorder," *Biol Psychiatry*, in press.
[7] G. Orrù, W. Petterson-Yeo, A. F. Marquand, G. Sartori, and A. Mechelli, "Using support vector machine to identify imaging biomarkers of neurological and psychiatric disease: A critical review," *Neurosci Biobehav Rev*, vol. 36, pp. 1140-1152, 2012.
[8] P. Fang, L.-L. Zeng, H. Shen L. Wang, B. Li, L. Liu, D. Hu, "Increased cortical-limbic anatomical network connectivity in Major Depression revealed by diffusion-tensor imaging." *PLoS One*, vol. 7, no. 9, pp. 1-10, 2012.
[9] M. Jenkinson, C. Beckmann, T. Behrens, M. Woolrich, and S. Smith, "FSL," *NeuroImage*, vol. 62, no. 2, pp. 782–790, 2012.
[10] G. Prasad, T. M. Nir, A. W. Toga, and P. M. Thompson, "Tractography density and network measures in Alzheimer's disease," *IEEE 10th International Symposium on Biomedical Imaging*, pp. 692-695, 2013.
[11] I. Aganj *et al.*, "A Hough transform global probabilistic approach to multiple-subject diffusion MRI tractography," *Medical Image Analysis*, vol. 15, no. 4, pp. 414-425, 2011.
[12] A. Klein *et al.*, "Evaluation of 14 nonlinear deformation algorithms applied to human brain MRI registration," *NeuroImage*, vol. 46, no. 3, pp. 786-802, 2009.
[13] B. A. Ardekani, S. Guckemus, A. Bachman, M. J. Hoptman, M. Wojtaszek, and J. Nierenberg, "Quantitative comparison of algorithms for inter-subject registration of 3D volumetric brain MRI scans," *J Neurosci Methods*, vol. 142, no. 1, pp. 67-76, 2005.
[14] O. Sporns, Networks of the Brain. The MIT Press, Cambridge, MA, 2011.
[15] Y. Benjamini, and Y. Hochberg, "Controlling the false discovery rate: A practical and powerful approach to multiple testing," *J Roy Stat Soc Ser B*, vol. 57, pp. 289-300.
[16] C. Hamani, H. Mayberg, S. Stone, A. Laxton, S. Haber, and A. M. Lozano, "The subcallosal cingulate gyrus in the context of major depression," *Biol Psychiatry*, vol. 69, pp. 301-308, 2011.